

Observations of viscous magnetization in multidomain magnetite

Adrian R. Muxworthy

Institute of Earth Science, University of Edinburgh, Edinburgh, UK

Southampton Oceanography Centre, School of Ocean and Earth Sciences, University of Southampton, Southampton, UK

Wyn Williams

Institute of Earth Science, University of Edinburgh, Edinburgh, UK

Received 24 June 2005; revised 28 September 2005; accepted 31 October 2005; published 27 January 2006.

[1] The viscous behavior of multidomain magnetite has been directly observed in both natural and synthetic samples using Bitter pattern imaging. A computer-controlled fully automated microscope fitted with a heating stage, field coils, and digital camera was used to record viscous acquisition and decay sequences as a function of time, temperature, and field. Domain walls (DW) were observed to move continuously through a series of quasi-static states over many hours rather than instantaneously. Viscosity was observed only on grains oriented near to the $\{111\}$ surface. Generally, DWs moved perpendicular to their surface in the direction of the applied field; however, because observed domains respond primarily to the movement of main domains underneath the surface, occasionally, DWs moved in the opposite direction to the applied field. Small variations in temperature were found to strongly influence the viscosity, supporting the idea that viscosity is thermally activated. Viscous and nonviscous domain structures were examined using magnetic force microscopy. These images revealed that the domains displaying viscous behavior tended to be narrow ($\sim 2 \mu\text{m}$ in width). Larger domains on grains oriented near the $\{111\}$ surface did not display viscosity, reflecting the greater energy required to move larger domain structures. This may explain why no viscosity was observed on the $\{110\}$ surfaces, as the domains were wider, that is, $\sim 6\text{--}10 \mu\text{m}$. A complex spiraling vortex-like magnetic domain structure was imaged. Etch pit analysis found a corresponding dislocation pit at the same location. It is suggested that this corresponds to the microstructure around a screw dislocation line.

Citation: Muxworthy, A. R., and W. Williams (2006), Observations of viscous magnetization in multidomain magnetite, *J. Geophys. Res.*, *111*, B01103, doi:10.1029/2005JB003902.

1. Introduction

[2] Viscous magnetization is a common time-dependent secondary component of natural remanent magnetization (NRM), and is known to significantly affect the accuracy and even the reliability of paleomagnetic results. Understanding viscous magnetization processes and the controlling mechanisms is therefore of fundamental importance to paleomagnetism, and has been much studied over the last 50 years.

[3] Viscous magnetizations can be due to switching of the magnetic moments in single-domain (SD) systems or the movement of domain walls in multidomain (MD) grains. Whether a system is said to be “viscous” or not, depends to a certain degree upon the timescale of interest; this may be of the order of a few picoseconds for people examining magnetic switching mechanisms or millions of years for geologists.

[4] There are various mechanisms that are thought to contribute to the viscous behavior in magnetic materials, but assuming no chemical alteration only two are thought to be significant for magnetite in the Earth’s field: (1) thermal fluctuations and (2) diffusion after-effects [Moskowitz, 1985]. For SD assemblages the thermal fluctuation theory of Walton [1980], which extended Néel’s [1949] theory to include grain distributions and magnetostatic interactions, has been experimentally shown to describe SD viscous behavior [Walton, 1983; Walton and Dunlop, 1985]. In contrast, MD viscous magnetization is less well described by thermal fluctuations theories [e.g., Néel, 1950, 1955; Stacey, 1963; Aver’yanov, 1967a, 1967b], and it appears to be controlled by a combination of both thermal fluctuations and diffusion after-effects [Tropin *et al.*, 1973; Moskowitz, 1985; Williams and Muxworthy, 2006]. The exact physical mechanisms responsible for MD viscosity, however, remain elusive.

[5] MD thermal fluctuation models assume that once a domain wall (DW) has reached a local energy minimum (LEM), it will remain there until a sufficiently large thermal

fluctuation event occurs for it to jump to a new LEM. These local energy minima are often related to pinning sites in the crystal structure, such as dislocation lines or impurities, and it possible for these pinning localities to move, especially at high temperatures [Weertman, 1978; Putnis, 1992], giving rise to DW movement. It is this diffusion effect, termed dislocation creep, which is commonly removed from samples by “thermal stabilization” [e.g., Sholpo *et al.*, 1991; Dunlop and Özdemir, 2000], achieved by heating a sample above the temperature of any future experiments. Another diffusion effect is disaccommodation, which is attributed to diffusive re-ordering of vacancies and ferrous ions [Néel, 1952; Walz, 2002]. The longer a sample has been in a steady field or zero field before a change in the field the greater the degree of diffusive re-ordering, the more strongly the domain walls are pinned and the smaller the viscous magnetization will be on application of a new field [Sholpo, 1967; Halgedahl, 1993]. There are a number of mechanisms controlling disaccommodation in magnetite, giving rise to a complex temperature dependency [Walz, 2002].

[6] As Moskowitz [1985] discussed, dislocation creep and thermal fluctuations, and disaccommodation contribute to viscosity in fundamentally different ways. Dislocation creep and thermal fluctuations cause a change in the pre-existing magnetization; that is, there is movement from one LEM state to another. Disaccommodation on the other hand causes a resistance to change; it hardens the magnetic structure [Trukhin, 1972]. Most previous MD viscosity investigations of naturally occurring minerals, have measured variations in magnetic moments [e.g., Shimizu, 1960; Sholpo, 1967; Shashkanov and Metallova, 1970; Dunlop, 1983; Williams and Muxworthy, 2006]. An exception to this is the work of Soffel [1976, 1979], who examined the possibility of viscous behavior in MD pyrrhotite through the direct observation of the magnetic domain structure using Bitter pattern imaging [Bitter, 1931]. However, his room temperature observations did not show any domain wall movements in a constant field.

[7] In this paper, we examine for the first time the magnetic viscosity of MD magnetite from direct Bitter pattern observations of magnetic domains as a function of time, temperature and field direction. In addition to the viscosity measurements we compare the Bitter pattern and high-resolution magnetic force microscope (MFM) images of the same grains made at room temperature. Finally, we compare the magnetic domain structures with dislocation localities determined by etch pit analysis.

2. Instrumentation

[8] The Bitter pattern technique was chosen for the majority of the viscosity observations over other higher-resolution methods, such as magnetic force microscopy (MFM), since we required: (1) “instantaneous” response to magnetic changes, rather than ~ 10 min to obtain an MFM image, (2) ability to vary temperature, (3) reliability, ease of use, and long-period stability (some observations lasted for more than one month) and (4) observations independent of imaging sensor, for example, a magnetized MFM tip can interact with and alter a sample’s magnetic structure [Foss *et al.*, 1997]. We will not discuss here the technicalities of the Bitter pattern method, as it is a standard tool and is well documented in the rock magnetic literature

[e.g., Soffel, 1965; Halgedahl and Fuller, 1980; Muxworthy and Heider, 2001].

[9] To assess the variation in viscosity with temperature, the samples were placed inside a sealed Linkam THMSG600 heating stage, which provides controlled heating up to 600°C. It was necessary to use long working distance (air) objectives to prevent conduction of heat from the stage to the lens, as small variations in lens temperature ($\sim 1^\circ\text{C}$) cause images to become quickly out of focus. To reduce problems of ferrofluid evaporation caused by heating, oil rather than water-based ferrofluids were used. A pair of field coils were set up next to the heating platform which could induce a uniform and controlled field up to 3 mT over the sample region, using a constant current source. As the system was fan-cooled (see below) the field coils did not heat significantly and the magnetic field was constant. To reduce the contribution of the Earth’s field, the entire microscope was placed within three Helmholtz coils. The field at the heating platform was reduced to $\sim 1 \mu\text{T}$. As the lenses were long-distance-working air objectives, they had no springs inside them, which can easily become magnetized (N. Pertersen, personal communication, 2003). Nevertheless the lenses and other parts of the heating platform were routinely alternating-field (AF) demagnetized. The viscosity observations were fully automated: a computer program was written to control the magnetic field, the temperature and the digital camera allowing for sequences of acquisition and decay observations to be made at various temperatures and fields. The longest sequence lasted over one month.

[10] There were some limitations with the system; the flash point of the ferrofluid was 212°C and was unstable at temperatures $>150^\circ\text{C}$ over extended periods of time. However, this modest increase in temperature was sufficient to initiate significant variation in domain wall mobility. For all the magnetite observations reported in this paper the temperature was $\leq 100^\circ\text{C}$. At these low temperatures the ferrofluid was stable and responsive for periods in excess of one month. Small variations in the temperature of the lenses ($\sim 1^\circ\text{C}$) were sufficient to cause the image to de-focus. The lens could be warmed because of (1) the heating platform, (2) field coils and (3) temperature variations in the laboratory over a period of days. Heat generated from the first two sources was removed by two cooling fans whose motors were placed outside the Helmholtz coil system. Temperature variations in the room were kept to a minimum. On a number of occasions the image remained in focus for more than two weeks without any adjustment.

[11] It is thought that the initial magnetic state of a sample is critical to viscosity experiments. For example disaccommodation effects have been shown to decrease viscosity rates as the zero-field waiting time is increased before viscosity measurements [Tivey and Johnson, 1981, 1984]. However, Halgedahl [1993] found that this zero-field waiting time was far more important than the initial demagnetization state; that is whether it was initially thermally or AF demagnetized. Pechnikov [1967] drew similar conclusions about the un-importance of a thermally or AF demagnetized starting state. Nevertheless, the samples were systematically AF demagnetized in three directions at room temperature prior to each experiment. The samples were then placed into the heating stage and heated to the required temperature. Even for small changes in temperature, such as attaining

Table 1. Bulk Physical, Chemical, and Magnetic Properties of the Two Samples^a

Sample Name	Grain Size, μm	$\mu_0 H_C$, mT	$\mu_0 H_{CR}$, mT	H_{CR}/H_C	M_{RS}/M_S	S_A/S_D	Chemical Description
<i>H</i> (32 μm)	32 (17)	0.9	22	24	0.005	1.1 ± 0.2	magnetite
<i>E</i> (150 μm)	150 (25)	1.9	17	8.7	0.02	1.0 ± 0.2	magnetite plus trace of hematite

^aThe grain size distributions for samples were determined from scanning electron micrographs. The grain size arithmetic means are shown, as are the standard deviations in parentheses. The chemical composition was determined from Mössbauer, X-ray diffraction, and magnetic analysis (this study and *Muxworthy and McClelland* [2000]). The viscosity data are taken from a study by *Williams and Muxworthy* [2006]. The viscosity ratio was determined from viscous remanent magnetization curves measured at 100°C (field = 2 mT). The S_A/S_D ratio for the hydrothermally produced sample is actually for a slightly smaller sample with a mean size of 23 μm , and the natural sample data are previously unpublished.

35°C from room temperature, the system took a significant amount of time to reach thermal equilibrium (~ 20 – 30 min). If an experiment was started within this time, the image would defocus relatively quickly. With the cooling fan system, this defocusing effect is unlikely to be due to heating of the lens. More likely it is due small thermal expansions and contractions of the sample and heating stage with temperature (N. Odling, personal communication, 2003), indicating that it takes a considerable amount of time for a sample to reach true thermal equilibrium. This 30 min equilibration time was therefore always performed before the experiments were started. A general feature of all MD thermal fluctuation theories [e.g., *Richter*, 1937; *Street and Woolley*, 1949; *Néel*, 1950, 1955; *Stacey*, 1963] is that the magnetization M is related to time t , as a first approximation by $M \propto \log(t)$, and so the digital time-lapse images were taken using logarithmic timescales.

[12] MFM images and the bulk magnetic hysteresis parameters were made at room temperature. MFM imaging is now a well developed technique, but issues related to image formation, interpretation and limitations of the method remain problematical [*Hubert and Schäfer*, 1998]. As with other studies [e.g., *Moloni et al.*, 1996; *Pokhil and Moskowitz*, 1997] the MFM images were made with the magnetic tip magnetized approximately perpendicular to the sample surface ($\sim z$ direction), making the MFM sensitive to the second derivative of the z component of the sample's stray field.

[13] For all domain observations, the crystallographic orientations of the grains were determined using a scanning electron microscope (SEM) fitted with electron backscatter diffraction (EBSD) facilities.

3. Samples

[14] We made observations on natural and synthetic magnetite samples (Table 1). Sample *H*(32 μm) was recently produced by hydrothermal re-crystallization [*Heider and Bryndzia*, 1987], and was stoichiometric magnetite. Natural sample *E*(150 μm) was collected from a green schist on the Shetland Isles, UK, and the magnetite crystals extracted from the rock matrix. Mössbauer spectroscopy and X-ray diffraction found that *E*(150 μm) contained traces of hematite [*Muxworthy and McClelland*, 2000]. The bulk magnetic properties of the two MD samples reported in the paper are also summarized in Table 1. The hysteresis data, in particular, the coercive force (H_C) data, suggest the hydrothermal sample had a very low concentration of dislocations. *E*(150 μm) has slightly higher H_C and coercivity of remanence (H_{CR}) compared to the synthetic sample.

[15] In a companion paper [*Williams and Muxworthy*, 2006], the magnetic viscosity behavior of sister samples is

reported. For bulk magnetic viscosity measurements, it is standard to plot the measured magnetization M versus time, t . As a first approximation M versus $\log(t)$ is a straight line and characteristic of the relaxation spectra. The gradient of this line is usually referred to as the viscosity coefficient S , where S_A and S_D represent the acquisition coefficients respectively. As a reference the ratio of S_A and S_D determined at 100°C for sister samples is shown in Table 1.

[16] For the Bitter pattern and MFM domain imaging the magnetite powders were dispersed in a non-magnetic, high-temperature epoxy, and then mechanically polished with diamond compounds. Amorphous silica solution was used as a final polish to obtain a smooth surface and to remove strain induced by the diamond polishing [*Hoffmann et al.*, 1987].

4. Domain Observations of Viscous Behavior

[17] For magnetite, the simplest domain patterns are observed on $\{110\}$ surfaces (Figure 1). On this surface the cubic magnetocrystalline anisotropy has two easy directions running parallel to the surface, so that both main (or body) and closure domains can be directly observed [e.g., *Özdemir et al.*, 1995; *Özdemir and Dunlop*, 1997]. For other orientations, the observed domain structures are primarily due to closure domains, leading to complex patterns. If only

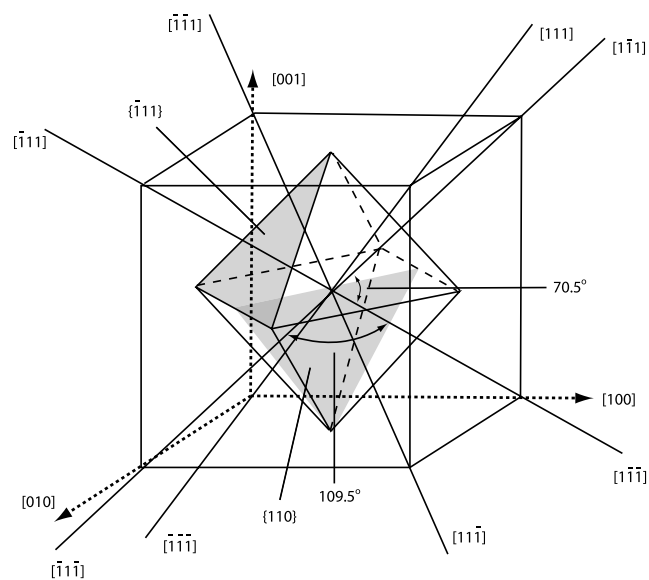


Figure 1. Schematic of a magnetite octahedron, showing the $\{110\}$ and $\{111\}$ planes and surfaces and the $\langle 110 \rangle$ and $\langle 111 \rangle$ directions.

closure domains are observed, their movement with time or temperature reflects primarily the behavior of hidden body domains beneath the surface. Closure domains are important in themselves, since, it has been argued that on cooling through the Verwey transition the contribution of closure domains is reduced giving rise to an increase in a remanence's measured magnetic moment [Muxworthy and Williams, 1999].

[18] Observing viscous behavior in magnetite grains proved to be exceptionally difficult. For a polished mount containing several hundreds of randomly oriented grains, the vast majority did not display any observed evidence for viscous behavior. In total 11 (out of several hundred examined) grains were found which displayed viscous behavior, all of which were oriented $<10^\circ$ from the $\{111\}$ surface (Figure 1). That more grains did not display viscous behavior does not mean that they would not under different conditions; simply no viscous behavior was observed on the one randomly oriented surface exposed to the camera. In addition grains whose surface stresses are not properly removed by polishing will also exhibit reduced viscosity. Because of the difficulty in observing viscous behavior, it was only after a grain had been observed displaying magnetic viscosity that its orientation was determined.

[19] In a recent paper [Williams and Muxworthy, 2006], we examined the influence of dislocation creep on viscosity rates by measuring viscosity before and after annealing the samples. That is, previously unheated samples, were heated to a new temperature and the viscosity immediately measured to assess the contribution of dislocation creep at this temperature. In this study no attempt was made to repeat this experiment, because in the search for viscous behavior the samples were typically heated to $\leq 100^\circ\text{C}$ several times before viscous behavior was observed. Therefore the observations reported here are not for "fresh" samples.

4.1. Hydrothermally Recrystallized Magnetites on a $\{111\}$ Surface

4.1.1. Viscous Acquisition

[20] The initial domain structure at 50°C of a grain *HA* from sample *H* ($32\ \mu\text{m}$) with size $\sim 62\ \mu\text{m}$ is shown in Figure 2a. The applied field is 2 mT, and the crystal is oriented $\sim 2^\circ$ from the $\{111\}$ surface and therefore demonstrates complex domain structure. The projections of the other three $\{111\}$ axes onto the $\{111\}$ -surface point in $\langle 112 \rangle$ directions. Because of the shape of the crystal it is straightforward to identify them (Figure 2d). The straight lines running across the whole sample are scratches on the grain surface.

[21] As the domain structure was observed over the next 24 hours, it gradually evolved through a sequence of domain wall (DW) movements. Initially these movements are small and at different localities on the surface (Figures 2a–2c). As time increased the number of DWs displaying viscosity increased, and the whole structure in the lower left area of the image moved. The behavior of two large DWs A and B is highlighted (Figure 2). The DW motion is not due to single instantaneous jumps, but instead DWs are seen to progress throughout the grain over periods of several hours, implying that viscosity is reflective of a grains' entire structure, rather than due to individual, independent DW movements. Simply put, the

domain walls move through a series of discrete quasi-static LEM states, and not through large instantaneous jumps. Generally DW motion is approximately perpendicular to the DW front in the direction closest to the field.

[22] Higher-resolution images were obtained by using an oil-objective lens but this was only useable at room temperature. However, it was more difficult to find grains displaying viscous behavior at a single temperature, so only a limited number of observations of this type were made. In Figure 3 grain *HA* was examined using the oil-objective lens to see if the fine domain wall structures, which could only be observed with the higher magnification, displayed viscosity at this lower temperature. Many of the fine intricate magnetic surface patterns are due to "quasi-domain" structures which form in minerals with cubic anisotropy as the magnetization vector is not confined to a plane [Abel, 1961; Hubert and Schäfer, 1998; Ambatiello *et al.*, 1999]. These are essentially multilayered closure domain structures, which become smaller toward the surface in attempt to accommodate the magnetic flux leakage (Figure 4). Each layer of closure domains gives rise to finer and finer domain structures [Ambatiello *et al.*, 1999], and in Figure 3, level 1 and level 2 structures have been identified. Furthermore slight misorientations of the grain surface also increase domain structure complexity [Hubert and Schäfer, 1998], and are therefore to be expected in grain *HA* which is oriented $\sim 2^\circ$ from the $\{111\}$ surface.

[23] These fine DW structures were found to display a higher degree of mobility than the larger domain structures (cf. Figures 2 and 3). The viscous behavior of three DWs marked A, B and C is highlighted over the sequence of images shown in Figure 3. Other DWs during this sequence move, but here we concentrate on the behavior of these three, in particular the back-and-forth motion of DW B. For the first 1226 s the grain displayed no viscous behavior at all. However, between 1226 s and 1330 s, DWs B and C moved toward the top left of the grain, partially in the direction of the applied field. Between 1330 s and 1444 s, DW C continues to move in the same direction, but DW B jumps back in the opposite direction. Between Figures 3c and 3d, again DW B moves back in the opposite direction to the applied field, with DWs A and C remaining fixed. Between 1705 s and 2390 s, DW C moves toward the top left, while DWs A and B move away from each other to increase the size of the domain between them. On increasing the time to 9914 s, it is seen that this domain has continued to increase in size, such that DWs B and C now touch each other. Between Figures 3e and 3f, DWs nucleate in the bottom left of the image.

[24] The finer DW structures are seen to readily display viscous behavior (Figure 3); however, this is likely to reflect DW movements deeper within the grain. That is, the finer domains' viscous behavior is most probably only in response to other deeper quasi-domain and/or body DW movements.

[25] Another example of viscous behavior is seen in Figure 5 for grain *HB* near the $\{111\}$ surface ($\sim 1^\circ$ off). The behavior is similar to that observed for *HA*. This image shows the difficulty in presenting such fine DW movements observed using the long-distance-working lens. To help highlight DW motion, Figure 5a was subtracted from Figure 5c to produce Figure 5b, and the resulting image shows DW movement (plus some noise) as dark stripes.

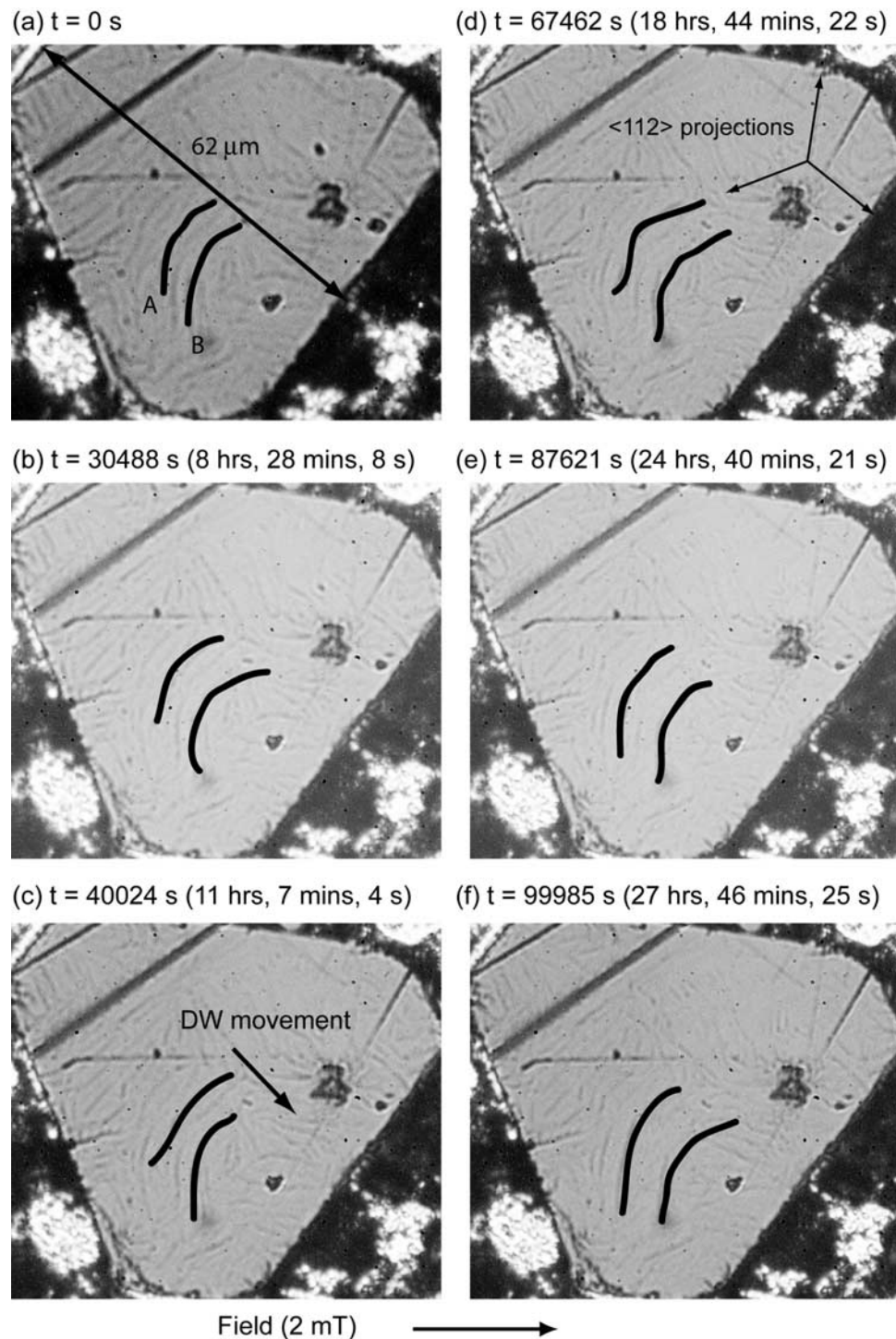


Figure 2. Bitter pattern images as a function of time for grain *HA* at 50°C. Grain *HA* was oriented $\sim 2^\circ$ from a $\{111\}$ plane and was initially AF demagnetized at room temperature. The applied field was 2 mT, and its direction is depicted. The $\langle 112 \rangle$ projections of the other three $\langle 111 \rangle$ axes are shown in Figure 2d.

The observed behavior of grain *HB* and others were similar to that of grain *HA*. That is, the domain structure as a whole moves through a series of wall movements rather than instantaneously. The domain walls move almost orthogonal to the field direction.

4.1.2. Repeatability and Initial Domain State

[26] The repeatability of the results observed in sections 4.1.1 was assessed, and it was quickly realized that the

initial observed domain state is critical to whether viscous effects were observed or not. After AF demagnetization, the domain structure of grain *HA* was typically in one of two general types; a diagonal state (Figure 6a) and a vertical state (Figure 6b) corresponding to two $\langle 112 \rangle$ directions, that is, projections of the closest $\langle 111 \rangle$ axes. By symmetry a third $\langle 112 \rangle$ direction would also be expected; however, presumably it is suppressed by the

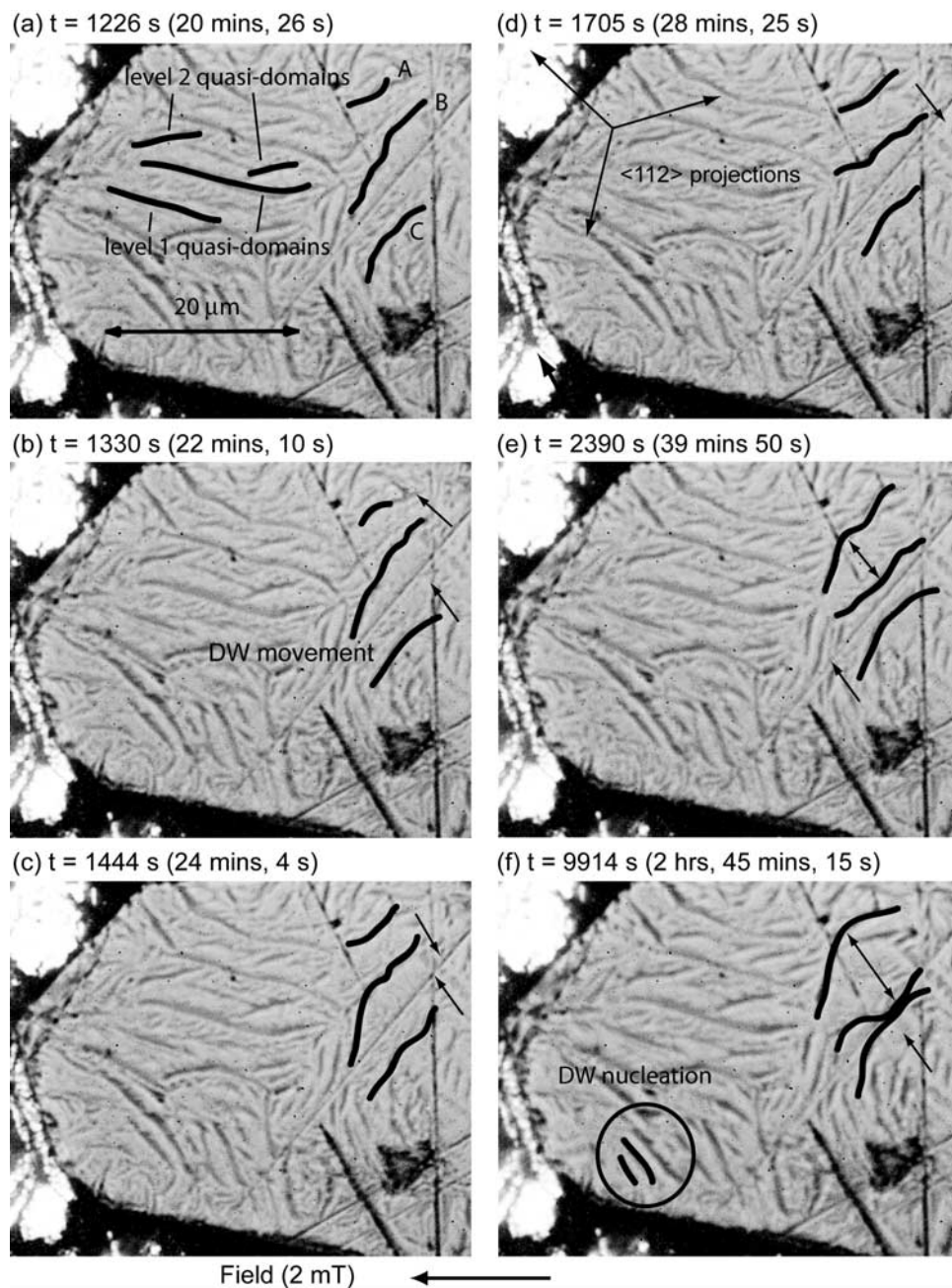


Figure 3. Oil emersion lens Bitter pattern images as a function of time for grain *HA* at 26°C. The behavior of three domain walls with time is highlighted. To increase resolution, the oil emersion lens was employed; however, this meant that only room temperature observations could be made. In Figure 3a, level 1 and level 2 quasi-domains are highlighted. Grain *HA* was oriented $\sim 2^\circ$ from a $\{111\}$ plane and was initially AF demagnetized at room temperature before heating. The applied field was 2 mT, and its direction is shown. The $\langle 112 \rangle$ projections of the other three $\langle 111 \rangle$ axes are shown in Figure 3d.

2° -tilt. Such behavior is in agreement with *Halgedahl* [1991], who observed that repeated AF demagnetization produced a distribution of domain states rather than one repeatable state.

[27] The initial diagonal state consistently displayed viscous behavior depending on temperature (26 time-temperature sequences), whereas, the initial vertical state, did not display any viscous behavior regardless of applied field direction during eight sequences of various lengths at several temperatures $< 70^\circ\text{C}$. Such reliance on the initial

structure suggests that viscous behavior is to a certain degree unrepeatable; however, the initial diagonal state was consistently found to display viscous behavior, although the exact DW movements themselves varied.

4.1.3. Viscous Decay

[28] In addition to observing acquisition of magnetization, we also observed the decay of this acquired magnetization. The ratio S_A/S_D of the viscous acquisition rate S_A and decay rate S_D allows for the comparison of acquisition and decay mechanisms. Most MD thermal fluctuation

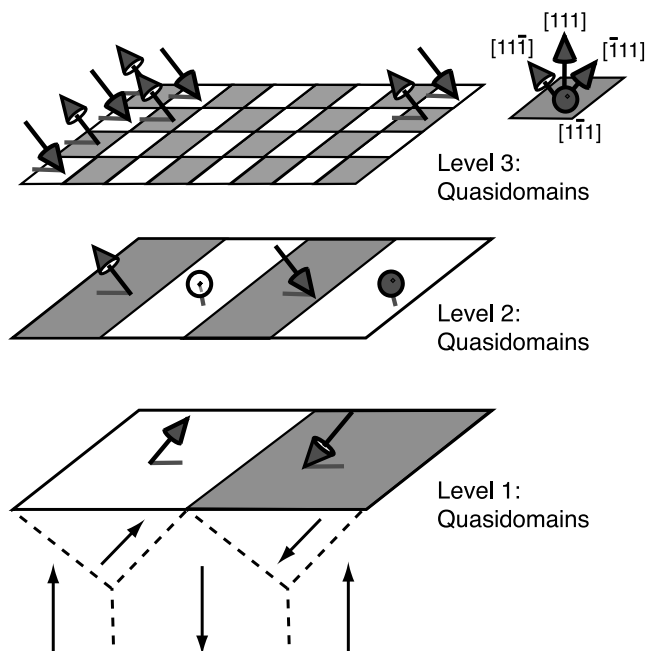


Figure 4. Schematic of a multilayered three-dimensional closure domain structures—quasi-domains. Such structures are possible in minerals like magnetite because, owing to the cubic magnetocrystalline anisotropy, the magnetization is not constrained to a plane [Ambatiello *et al.*, 1999]. The quasi-domains form to reduce the stray field on the $\{111\}$ plane. Each area of the checkered pattern (level 3) describes a homogeneous magnetization area (domain). The polar components of the magnetization average out, in contrast to the planar components. The net magnetizations of the planar components are compensated for by the level 1 and 2 quasi-domains. Below level 1, the bulk domain structure is depicted by the arrows and dotted lines. With the relatively low magnifications in this study, only the level 1 and 2 structures were observed, the structures associated with level 3 being too fine in detail. Redrawn after Ambatiello *et al.* [1999] with permission from Elsevier.

theories predict $S_A/S_D = 1$ [Richter, 1937; Street and Woolley, 1949; Stacey, 1963]. In contrast, Néel's [1950] thermal fluctuation model predicts $S_A/S_D = 2$.

[29] Because of the complex domain movements involved during viscous acquisition (Figure 2) and the partially unrepeatable nature of the viscosity observations, it is difficult to accurately quantify S_A/S_D from the observations; however, a qualitative zero-order approximation is cautiously made for individual domain walls on the basis of observations. In a repeat of the experiment in section 4.1.1, for grain *HA* at 50°C , a DW movement was identified during acquisition with a corresponding (reverse) DW movement during decay. The degree of DW movement in this sequence was less than that observed in Figure 2. The acquisition event occurred between 64653 s and 69910 s, that is, ~ 67000 s (~ 18 hrs), and the decay event between 155830 s and 180311 s, that is, ~ 168000 s (~ 46 hrs), making $S_A/S_D \approx 2.5$. That for this single DW event, $S_A/S_D < 2$, is consistent with Néel's [1950] thermal fluctuation theory. It is arguably justified to directly apply Néel's [1950] theory for a single DWs, as this observation corresponds to a single DW movement. This value of 2.5 is significantly higher than the magnetic estimate for S_A/S_D for an assemblage of similar grains at 100°C (Table 1). However, it is difficult to draw comparisons because of the statistical nature of S_A/S_D [Walton, 1980; Williams and Muxworthy, 2006].

4.1.4. Variation in Applied Field

[30] In a similar experiment to those reported in sections 4.1.1 and 4.1.3, viscous acquisition in grain *HA* was observed at 50°C in a field of 3 mT. A DW event was recorded in the forward direction at ~ 66000 s. After 78050 s, the field direction was reversed, with the switching period taking ~ 2 s. On reversing the field, the same DW moved back in approximately the same time after switching the field direction, that is, ~ 88000 s. However, it is difficult to directly compare these two DW movements since other DW movements occurred in the vicinity during the forward field observation, but did not move during the reverse field

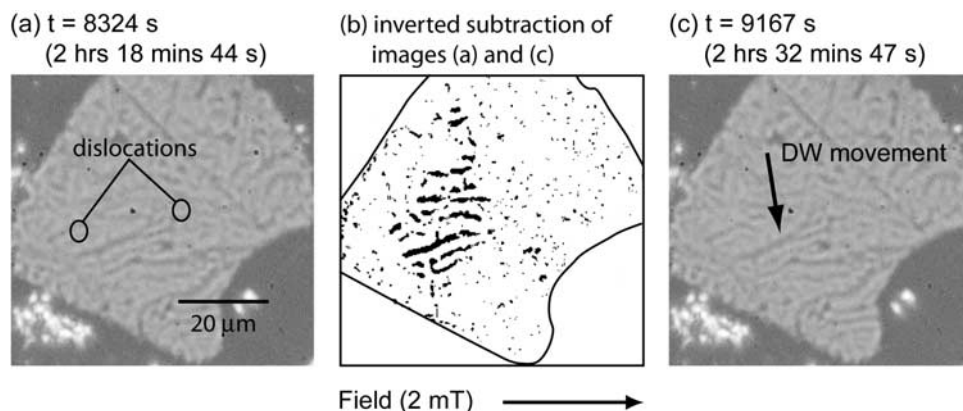


Figure 5. (a and c) Two Bitter pattern images as a function of time for grain *HB* at 60°C . (b) Inverted difference between Figures 5a and 5c; this highlights domain wall movement, in addition to some noise. In Figure 5a, two dislocations are highlighted. The positions of these were determined by etch pit analysis (section 6). Grain *HB* was oriented $\sim 1^\circ$ from a $\{111\}$ plane and was initially AF demagnetized at room temperature before heating. The applied field was 2 mT, and its direction is shown.

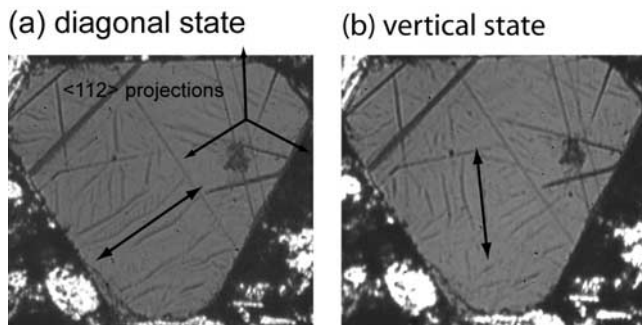


Figure 6. Bitter pattern images of grain *HA* at room temperature for two initial starting states after AF demagnetization with no applied field. Grain *HA* was oriented $\sim 2^\circ$ from a $\{111\}$ plane. The $\langle 112 \rangle$ projections of the other three $\langle 111 \rangle$ axes are shown in Figure 6a.

observation, and *vice versa*, suggesting that DWs do not behave individually but interact with one another.

4.1.5. Temperature Variation

[31] The effect of varying temperature on the viscosity rates was examined. A key feature that was repeatedly observed for all the grains displaying viscosity was that the temperature range over which a DW displayed significant mobility and viscous behavior was narrow. If a DW was found to display viscous behavior at a given temperature, say 50°C , then on heating to 55°C the DW rapidly became invisible. On cooling by $\sim 5^\circ\text{C}$, that is, to 45°C , the same DW no longer displayed viscous behavior on an observable timescale. This suggests that DWs displaying viscosity are associated with low-flux leakage structures, while energetically unfavorable and visible DWs not displaying viscosity (strongly pinned) are due to high-flux leakage structures. For example, on cooling *HA* in Figure 2 to 45°C , the viscosity behavior discussed in section 4.1.1 was greatly reduced. For sample *HA* at room temperature, it was only on using high-resolution oil emersion lenses that viscous behavior could be observed.

[32] These observations support the idea of thermally activated DW blocking, which is central to Néel's [1955] multidomain theory of thermoremanence acquisition. However, unlike Néel's [1955] model for a single DW, it would appear that the walls strongly interact with each other and that the entire domain structure, or at least significant volumes of a domain structure, are blocked rather than individual DWs. Even though temperature variations were extensively investigated, this variation in viscosity rate with temperature may also be associated with observations being only partially repeatable.

4.2. Natural Magnetite Oriented on the $\{111\}$ Direction

[33] Viscosity was observed on grain *DA* from sample *E* ($150\ \mu\text{m}$) (Figure 7) at 40°C . The grain was oriented $\sim 9^\circ$ from the $\{111\}$, giving rise to complex domain structures. In this sequence the DW movements were continuous and gradual over the entire duration of the acquisition period, that is, $\sim 86417\ \text{s}$ (24 hrs 1 min 11 s). In Figure 7 two images from the sequence, and the difference between the images are shown. The DWs near the right hand side of the grain move normal to the wall in the direction of the field. On heating to 45°C domain wall movements similar to those observed at 40°C were found, though the number of viscous DWs was less and the time at which they moved reduced. For example wall A marked in Figure 6a, first moved between $75496\ \text{s}$ and $79155\ \text{s}$ at a temperatures of 40°C , but on warming to 45°C the same wall first moved between $40700\ \text{s}$ and $44754\ \text{s}$. A decay event was observed for wall A at 45°C between $49214\ \text{s}$ and $54119\ \text{s}$, giving a single DW estimate $S_A/S_D \approx 1.2$. On heating to 50°C DW A was difficult to observe.

5. Comparison of Bitter Pattern and MFM Images

[34] To try to better understand the nature of the domain walls displaying viscous behavior, MFM imaging was performed at room temperature on a number of samples.

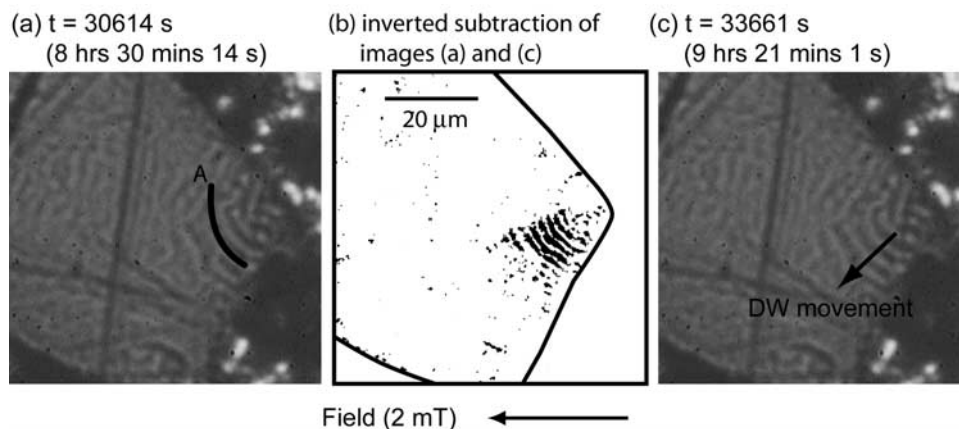


Figure 7. (a and c) Two Bitter pattern images at different times during viscous acquisition for grain *DA* at 40°C . Figure 7b shows the difference between Figures 7a and 7c; this image highlights domain wall movement (in addition to some noise). Grain *DA* was oriented $\sim 9^\circ$ from a $\{111\}$ plane and was initially AF demagnetized at room temperature before heating. The applied field was $2\ \text{mT}$, and its direction is shown.

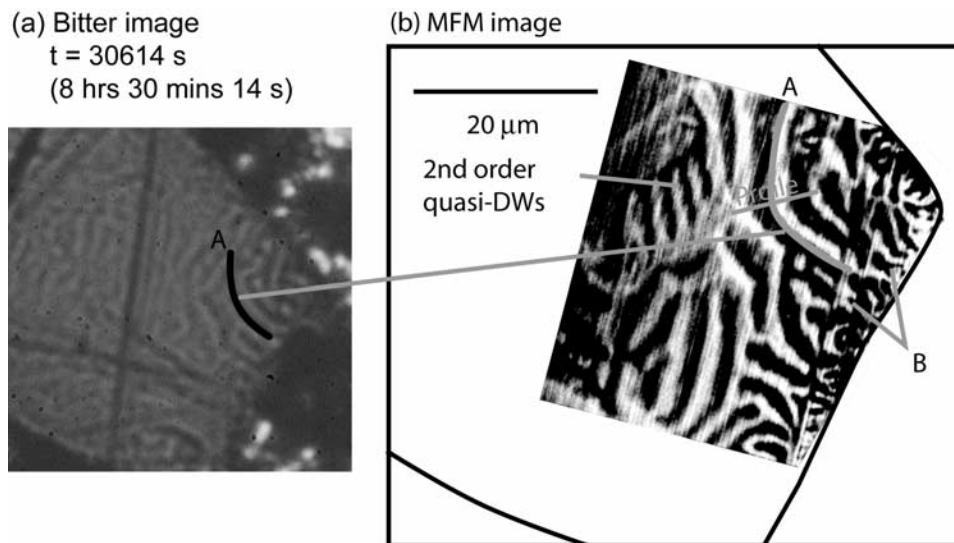


Figure 8. (a) Bitter pattern image and (b) MFM image for the same region of grain *DA*. The Bitter pattern image is the same as in Figure 7a; that is, the sample is at 40°C during a viscous acquisition experiment. The MFM image was taken at room temperature in the Earth’s field and was initially AF demagnetized. DW A is identified in both images. In Figure 8b, the complex domains which form where DW A meets with the surface are marked by B. DWs from second-order quasi-domain structures are highlighted. Grain *DA* was oriented $\sim 9^\circ$ from a $\{111\}$ plane.

Grain *HA* had previously undergone etch pit analysis (section 6) which meant that it was no longer suitable for MFM imaging.

5.1. Domain Walls Displaying Viscous Behavior

[35] For grain *DA*, the DWs which displayed viscous behavior were directly observed using MFM imaging (Figure 8). The magnetic pattern is quite complex because of the orientation of the grain $\sim 9^\circ$ from the $\{111\}$ plane; however, the general features are similar to those seen in the Bitter pattern image, that is, curved domain walls as highlighted by DW A. Fine domain structures related to level two quasi-domain structures are identified in Figure 8b. DW A and its surrounding domains showed significant viscous behavior. What is immediately apparent is that DW A itself is surrounded by a number of similar curved DWs and domains, and despite being curved the domains run parallel to each other. DW A is connected at surfaces of the grain by complex domain structures (marked by B in Figure 8b) rather than classic closure domain structures observed when the grain is oriented on the $\{110\}$ plane [e.g., Özdemir *et al.*, 1995]. DW B and its surrounding domains are quite narrow. Taking a straight profile as shown in Figure 8b gives an average domain width of $\sim 2 \mu\text{m}$.

5.2. Domain Walls Not Displaying Viscosity

5.2.1. Hydrothermally Recrystallized Magnetite on a $\{111\}$ Surface

[36] Another grain *HC* oriented $\sim 2^\circ$ off the $\{111\}$ surface, did not display viscous behavior. As stated previously there were many domain structures which did not display any viscous movement. The main domain structures are quite simple and regular, terminating in more complex structures at the grain surface (Figure 9a). For a comparison a sketch of the

observed Bitter pattern image is made in Figure 9b. The Bitter pattern image compares favorably with the MFM image, suggesting that the Bitter pattern imaging accurately depicts the large-scale features and their magnetic behavior. By taking a profile through the main domains (Figure 9a), as in section 5.1, the average domain width is observed as $< 5 \mu\text{m}$. This is significantly larger than for domains with similar orientation displaying viscous behavior.

5.2.2. Hydrothermally Recrystallized Magnetite on a $\{110\}$ Surface

[37] For comparison with the grains oriented on the $\{111\}$ surface we compare a hydrothermally recrystallized grain *HD* oriented near the $\{110\}$ surface; off by $\sim 11^\circ$ (Figure 10). The main domain structures are quite simple, with large central domains (Figure 10a). Two domain widths are highlighted, that is, $7.4 \mu\text{m}$ and $7.8 \mu\text{m}$, which are larger than the domain structures observed on $\{111\}$ surfaces (Figures 8 and 9). A schematic of the domain structure is shown in Figure 10b. As the crystal surface is misoriented by $\sim 11^\circ$ the moments do not run parallel to the surface, but dip slightly in to and out of the plane. Two “classic” closure domains are identified, but generally the edges of the grain displayed complex fine domain structures. In addition to the slight surface misorientation contributing to such features, over-polishing of the sample can also give rise to such edge effects, due to different degrees of hardness of the epoxy and magnetite. The interpretation of MFM images can be complicated by surface charges [Hubert *et al.*, 1997], in addition to which the actual directions of magnetization cannot be unambiguously determined by the MFM. In the schematic in Figure 10b, it is possible that all the domain magnetizations are oriented in the other direction; that is, the horizontal component of the magnetization rotates through 180° .

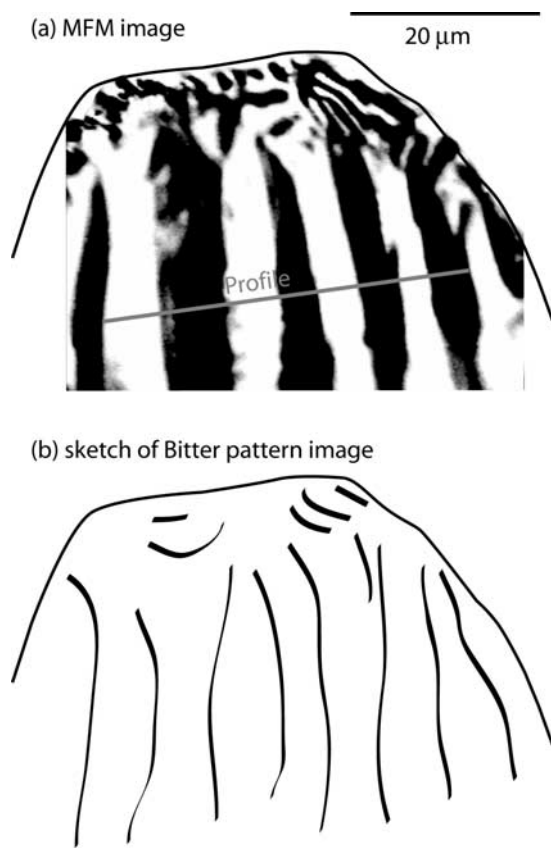


Figure 9. (a) MFM image of grain *HC* at room temperature in the Earth's field and (b) sketch of the Bitter pattern image observed at the same temperature. This grain, oriented $\sim 2^\circ$ from a $\{111\}$ plane, was not observed to display viscous behavior. Its grain size was $\sim 70 \mu\text{m}$. There is good correlation between the Bitter pattern image structure and that derived from MFM imaging. The domains are noticeably larger than the domains which displayed viscous behavior in Figure 8. The grain was initially AF demagnetized.

[38] Several domain wall profiles were made (Figures 10c and 10d). Profiles A and B correspond to 180° Bloch DWs for slightly misoriented domains [Pokhil and Moskowitz, 1996]. That profile A's DW is black and profile B's white, supports Pokhil and Moskowitz's [1997] findings for small magnetite crystals that domains and DWs interlink to give a consistent whole-grain chirality; that is, the magnetization in DWs rotate alternately upward and downward. Profiles C and D for 71° DWs are of poor quality; however, they both show consistent trends. If the magnetization in the domains is pointing slightly below the surface, the DW moments rotate out of the plane to give a positive signal. The opposite is true for DWs between domains with out-of-plane magnetization vectors.

[39] In agreement with other studies of MD magnetite [e.g., Pokhil and Moskowitz, 1996, 1997; Foss et al., 1998], on grains oriented near the $\{110\}$ surface zigzag domain wall patterns were observed, which contained Bloch lines separating each zigzag segment. The zigzag angles were of the order 10° – 50° . Of particular interest was a fine domain structure observed using the MFM (Figure 10e). It

is postulated that this feature corresponds to the magnetic structure observed around a screw dislocation line meeting the surface. Spiraling magnetic structures, as observed in Figure 10e, are predicted theoretically for screw dislocations [Shive, 1969].

6. Dislocations, Magnetic Structures, and Viscosity

[40] In an attempt to examine the relationship between dislocation structure and magnetic structures, etch pit analysis was performed on the samples after domain observations had been made. Etching was simply done by applying 40% HCl to magnetite surfaces for 30 s [Sahu, 1997]. The HCl preferentially removes magnetite where dislocation lines meet the surface. The resulting images show etch pits which reflect the locality of dislocations.

[41] Generally samples displaying viscous behavior had very low dislocation densities, for example, no etch pits were observed in the areas of grains *DA* and *HA* which showed viscous behavior. Sample *HC* displayed two etch pits near the vicinity of domain wall viscosity (Figure 5a). In this case the DW viscous behavior appears to move between the two dislocations. The very low dislocation densities generally observed in the vicinity of the viscous domains, suggests that viscous behavior is not due to dislocation creep, but rather thermal fluctuations. Etching of sample *HD* produced a pit in exactly the same locality as the spiral domain structure observed using the MFM (Figure 10e), adding support to the argument that this feature was due to a screw dislocation.

7. Discussion and Conclusions

[42] All the domain structures observed to display viscous behavior were on surfaces oriented near the $\{111\}$ plane. Generally, the DWs moved in response to the applied field direction, but some DWs were also observed to move in other directions, that is, the DWs responded to local interaction fields and energy states, and moved collectively. Domain wall movement was not instantaneous, occurring instead through a sequence of steps over many hours, moving between quasi-static local energy minima. For any given grain the general behavior was found to be repeatable, but specific DW structures and movements unrepeatable. The initial starting state was found to be critical to viscous behavior.

[43] Only a few dislocations were observed through etching, and there was no clear relationship between the observed dislocations and viscosity, unless of course the absence of dislocations increases viscous behavior. The low dislocation densities agree with the bulk magnetic hysteresis which had very low coercive force distributions.

[44] As the structures were observed on $\{111\}$ planes the DW structures were due to closure domains and quasi-domain structures, and difficult to interpret. Widths of domains and DWs displaying viscosity were narrower than those that did not display viscous behavior. Clearly movement of large domain structures will involve greater energies, and hence greater energy barriers will have to be surmounted for large domain structures to move. Viscosity would therefore appear to be more favorable in smaller

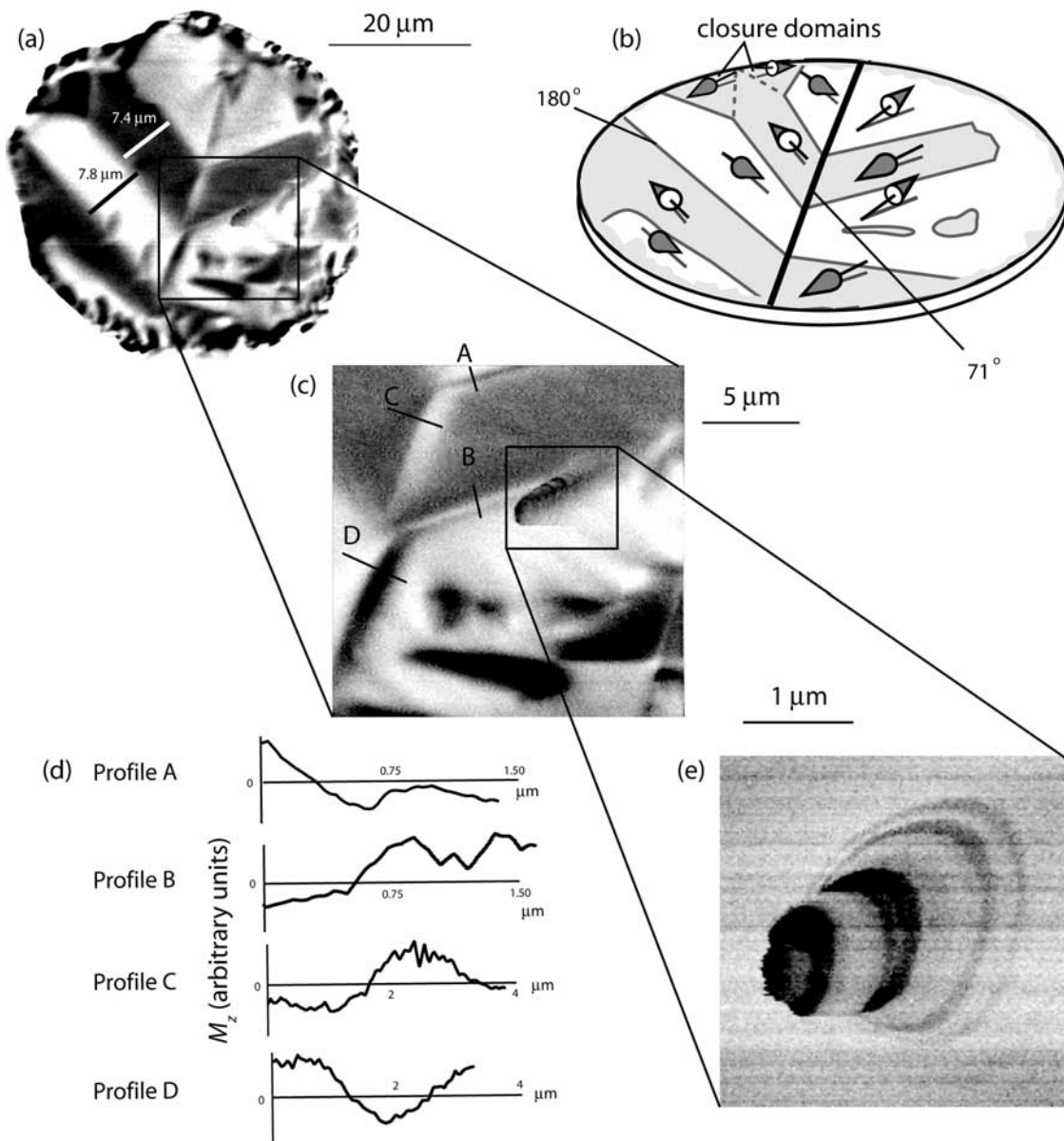


Figure 10. Series of MFM images of grain *HD* at room temperature in the Earth's field. The resolution of the images increases from top left (Figure 10a) to bottom right (Figure 10e). A schematic interpretation of the domain structure is shown in Figure 10b. Four DW profiles highlighted in Figure 10c are shown in Figure 10d. The image in Figure 10e is thought to be the magnetic structure around a screw dislocation. This grain was oriented $\sim 9^\circ$ from a $\{110\}$ plane and was not observed to display viscous behavior. The widths of two domains are highlighted in Figure 10a. The grain was initially AF demagnetized.

domains. Domain widths observed on the $\{110\}$ plane were larger than those observed on $\{111\}$ surface, which may partially explain why no viscosity was observed. It may also be that only quasi-closure domain structures display viscosity. These observations support a thermal fluctuation model of viscous behavior. The observations provide no evidence for dislocation creep contributing to viscous behavior [Williams and Muxworthy, 2006]. However, as the samples had been heated many times and effectively annealed, then dislocation creep would not be expected to be observed.

[45] DWs displayed viscous behavior over a very narrow temperature range, that is, $\sim 15^\circ\text{C}$. As the temperature was

increased the walls became more viscous, but also less visible, eventually disappearing.

[46] Estimates of the S_A/S_D for individual DWs were made with great variations in values ranging from 1–2.5. Because of the wide range in S_A/S_D ratios and the unrepeatable nature of the DW movement, it is difficult to assess which MD thermal fluctuation model is best described by the data. However, as all the thermal fluctuation models are based on single DW movements and observations indicate that DWs behave collectively, then it would appear that none of the models will be explicitly correct.

[47] Collective DW behavior may partially explain why Néel's [1955] MD thermoremanence theory fails

[e.g., McClelland and Sugiura, 1987; Sholpo et al., 1991; Muxworthy, 2000], as the model is for an individual DW, when in reality domains and DWs do not behave individually. As the local energy state of a DW wall would vary with each neighboring DW movement, then this would lead to a thermoremanence acquisition on a bulk scale becoming essentially a statistical problem [Fabian, 2003; Fabian and Shcherbakov, 2004].

[48] An MFM image of a spiraling magnetic structure occurred where etching revealed a dislocation line reaching the surface. This structure would appear to be in agreement with analytical calculations for the interaction of the magnetization with a screw dislocation [Shive, 1969].

[49] **Acknowledgments.** This work was funded through NERC research grant NER/A/S/2001/00539 to W.W. A.R.M. is funded by the Royal Society. A visiting fellowship to the Institute for Rock Magnetism (IRM), University of Minnesota, is gratefully acknowledged. The IRM is funded by the National Science Foundation, W. M. Keck Foundation, and the University of Minnesota. We would like to thank Heinrich Soffel for sending us a copy of his film which he presented at EGS 1976 and IUGG 1979. We would like to thank Nic Odling for his help with the hydrothermal recrystallization technique. We would also like to thank John Craven, Nic Odling, Nicola Crazer, and David Krása for their help and suggestions with the microscopy and sample preparation.

References

- Abel, V. R. (1961), The grouping of magnetic regions in silicon sheet iron, *Phys. Meteorol. Metallogr.*, *11*, 353–359.
- Ambatiello, A., K. Fabian, and V. Hoffmann (1999), Magnetic domain structure of multidomain magnetite as a function of temperature: Observation by Kerr microscopy, *Phys. Earth Planet. Inter.*, *112*, 55–80.
- Aver'yanov, V. S. (1967a), Contribution to the theory of the thermally activated magnetic viscosity of multidomain particles of ferromagnetic materials 2, *Izv. Russ. Acad. Sci. Phys. Solid Earth*, Engl. Transl., *9*, 592–595.
- Aver'yanov, V. S. (1967b), Contribution to the theory of the thermally activated magnetic viscosity of multidomain particles of ferromagnetic materials 1, *Izv. Rus. Acad. Sci. Phys. Solid Earth*, Engl. Transl., *8*, 531–536.
- Bitter, F. (1931), On inhomogeneities in the magnetization of ferromagnetic materials, *Phys. Rev.*, *38*, 1903–1905.
- Dunlop, D. J. (1983), Viscous magnetization of 0.04–100 micron magnetites, *Geophys. J. R. Astron. Soc.*, *74*, 667–687.
- Dunlop, D. J., and Ö. Özdemir (2000), Effect of grain size and domain state on thermal demagnetization tails, *Geophys. Res. Lett.*, *27*, 1311–1314.
- Fabian, K. (2003), Statistical theory of weak field thermoremanent magnetization in multidomain particle ensembles, *Geophys. J. Int.*, *155*, 479–488.
- Fabian, K., and V. Shcherbakov (2004), Domain state stabilization by iterated thermal magnetization processes, *Geophys. J. Int.*, *159*, 486–494.
- Foss, S., E. D. Dahlberg, R. Proksch, and B. M. Moskowitz (1997), Measurement of the effects of the localized field of a magnetic force microscope tip on a 180 degree domain wall, *J. Appl. Phys.*, *81*, 5032–5034.
- Foss, S., B. M. Moskowitz, R. Proksch, and E. D. Dahlberg (1998), Domain wall structures in single-crystal magnetite investigated by magnetic force microscopy, *J. Geophys. Res.*, *103*, 30,551–30,560.
- Halgedahl, S. L. (1991), Magnetic domain patterns observed on synthetic Ti-rich titanomagnetite as a function of temperature and in states of thermoremanent magnetization, *J. Geophys. Res.*, *96*, 3943–3972.
- Halgedahl, S. L. (1993), Experiments to investigate the origin of anomalously elevated unblocking temperatures, *J. Geophys. Res.*, *98*, 22,443–22,460.
- Halgedahl, S. L., and M. Fuller (1980), Magnetic domain observations of nucleation processes in fine particles of intermediate titanomagnetite, *Nature*, *288*, 70–72.
- Heider, F., and L. T. Bryndzia (1987), Hydrothermal growth of magnetite crystals (1 μm to 1 mm), *J. Cryst. Growth*, *84*, 50–56.
- Hoffmann, V., R. Schäfer, E. Appel, A. Hubert, and H. Soffel (1987), First domain observations with the magneto-optical Kerr effect of Ti-ferrites in rocks and their synthetic equivalents, *J. Magn. Magn. Mater.*, *71*, 90–94.
- Hubert, A., and R. Schäfer (1998), *Magnetic Domains*, Springer, New York.
- Hubert, A., W. Rave, and S. L. Tomlinson (1997), Imaging magnetic charges with magnetic force microscopy, *Phys. Status Solidi B*, *204*, 817–828.
- McClelland, E., and N. Sugiura (1987), A kinematic model of TRM acquisition in multidomain magnetite, *Phys. Earth Planet. Inter.*, *46*, 9–23.
- Moloni, K., B. M. Moskowitz, and E. D. Dahlberg (1996), Domain structures in single-crystal magnetite below the Verwey transition as observed with a low-temperature magnetic force microscope, *Geophys. Res. Lett.*, *23*, 2851–2854.
- Moskowitz, B. M. (1985), Magnetic viscosity, diffusion after-effect and disaccommodation in natural and synthetic samples, *Geophys. J. R. Astron. Soc.*, *82*, 143–161.
- Muxworthy, A. R. (2000), Cooling behaviour of partial thermoremanences induced in multidomain magnetite, *Earth Planet. Sci. Lett.*, *184*, 149–159.
- Muxworthy, A. R., and F. Heider (2001), Rock magnetic investigation of historical lavas used in palaeointensity studies, *Stud. Geophys. Geod.*, *45*, 283–296.
- Muxworthy, A. R., and E. McClelland (2000), The causes of low-temperature demagnetization of remanence in multidomain magnetite, *Geophys. J. Int.*, *140*, 115–131.
- Muxworthy, A. R., and W. Williams (1999), Micromagnetic models of pseudo-single domain grains of magnetite near the Verwey transition, *J. Geophys. Res.*, *104*, 29,203–29,217.
- Néel, L. (1949), Théorie du traînage magnétique des ferromagnétiques en grains fins avec applications aux terres cuites, *Ann. Geophys.*, *5*, 99–136.
- Néel, L. (1950), Théorie du traînage magnétique des substances massives dans le domaine de Rayleigh, *J. Phys. Radium*, *11*, 49–61.
- Néel, L. (1952), Théorie du traînage magnétique de diffusion, *J. Phys.*, *13*, 249–254.
- Néel, L. (1955), Some theoretical aspects of rock magnetism, *Adv. Phys.*, *4*, 191–243.
- Özdemir, Ö., and D. J. Dunlop (1997), Effect of crystal defects and internal stress on the domain structure and magnetite properties of magnetite, *J. Geophys. Res.*, *102*, 20,211–20,224.
- Özdemir, Ö., S. Xu, and D. J. Dunlop (1995), Closure domains in magnetite, *J. Geophys. Res.*, *100*, 2193–2209.
- Pechnikov, V. S. (1967), On the time variation of magnetic viscosity, *Izv. Russ. Acad. Sci. Phys. Solid Earth*, Engl. Transl., *6*, 413–415.
- Pokhil, T. G., and B. M. Moskowitz (1996), Magnetic force microscope study of domain wall structures in magnetite, *J. Appl. Phys.*, *79*, 6064–6066.
- Pokhil, T. G., and B. M. Moskowitz (1997), Domains and domain walls in pseudo-single-domain magnetite studied with magnetic force microscopy, *J. Geophys. Res.*, *102*, 22,681–22,694.
- Putnis, A. (1992), *Introduction to Mineral Sciences*, 457 pp., Cambridge Univ. Press, New York.
- Richter, G. (1937), Über die magnetische Nachwirkung am Carboneyleisen, *Ann. Phys.*, *29*, 605–635.
- Sahu, S. (1997), An experimental study on the effects of stress on the magnetic properties of magnetite, Ph.D. thesis, Univ. of Minn., Minneapolis.
- Shashkanov, V. A., and V. V. Metallova (1970), Temperature dependence of the magnetic viscosity coefficient, *Izv. Russ. Acad. Sci. Phys. Solid Earth*, Engl. Transl., *7*, 457–459.
- Shimizu, Y. (1960), Magnetic viscosity of magnetite, *J. Geomagn. Geoelectr.*, *11*, 125–138.
- Shive, P. N. (1969), Dislocation control of magnetisation, *J. Geomagn. Geoelectr.*, *21*, 519–529.
- Sholpo, L. Y. (1967), Regularities and methods of study of the magnetic viscosity of rocks, *Izv. Russ. Acad. Sci. Phys. Solid Earth*, Engl. Transl., *6*, 390–399.
- Sholpo, L. Y., V. A. Ivanov, and G. P. Borisova (1991), Thermomagnetic effects of reorganization of domain structure, *Izv. Russ. Acad. Sci. Phys. Solid Earth*, Engl. Transl., *27*, 617–623.
- Soffel, H. (1965), Magnetic domains of polycrystalline natural magnetite, *Z. Geophys.*, *31*, 345–361.
- Soffel, H. (1976), Magnetic domains of natural pyrrhotite in a Devonian diabase from northern Bavaria, Germany, paper presented at 3rd General Assembly, Eur. Geophys. Soc., Amsterdam.
- Soffel, H. (1979), Magnetic domains of natural pyrrhotite in a Devonian diabase from northern Bavaria, Germany, paper presented at 14th General Assembly, Int. Union of Geod. Geophys., Canberra.
- Stacey, F. D. (1963), The physical theory of rock magnetism, *Adv. Phys.*, *12*, 45–133.
- Street, R., and J. C. Woolley (1949), A study of magnetic viscosity, *Proc. Phys. Soc. London, Sect. A*, *62*, 562–572.
- Tivey, M. A., and H. P. Johnson (1981), Characterization of viscous remanent magnetization in single- and multidomain magnetite grains, *Geophys. Res. Lett.*, *8*, 217–220.

- Tivey, M. A., and H. P. Johnson (1984), The characterization of viscous remanent magnetization in large and small magnetite particles, *J. Geophys. Res.*, *89*, 543–552.
- Tropin, Y. D., I. M. Belous, and I. A. Stretskul (1973), On the thermally activated magnetic viscosity of rocks, *Izv. Russ. Acad. Sci. Phys. Solid Earth*, Engl. Transl., *1*, 61–62.
- Trukhin, V. I. (1972), Interpretation of data on the magnetic viscosity of rocks, *Izv. Russ. Acad. Sci. Phys. Solid Earth*, Engl. Transl., *4*, 235–241.
- Walton, D. (1980), Time-temperature relations in the magnetisation of assemblies of single domain grains, *Nature*, *286*, 245–247.
- Walton, D. (1983), Viscous magnetization, *Nature*, *305*, 616–619.
- Walton, D., and D. J. Dunlop (1985), The magnetisation of a random assembly of interacting moments, *Solid State Commun.*, *53*, 359–362.
- Walz, F. (2002), The Verwey transition—A topical review, *J. Phys. Condens. Matter*, *14*, R285–R340.
- Weertman, J. (1978), Creep laws for the mantle of the Earth, *Philos. Trans. R. Soc. London, Sect. A*, *288*, 9–22.
- Williams, W., and A. R. Muxworthy (2006), Understanding viscous magnetization of multidomain magnetite, *J. Geophys. Res.*, doi:10.1029/2005JB003695, in press.

A. R. Muxworthy, Southampton Oceanography Centre, School of Ocean and Earth Sciences, University of Southampton, European Way, Southampton SO14 3ZH, UK. (adrian.muxworthy@gmail.com)

W. Williams, Institute of Earth Science, University of Edinburgh, Kings Buildings, West Mains Road, Edinburgh EH9 3JW, UK.